



Sveriges lantbruksuniversitet
Swedish University of Agricultural Sciences

**Faculty of Veterinary Medicine
and Animal Science**
Department of BVF

Assessing the ability of LARGE overexpression to prevent the development of muscular dystrophy

Astrid Rudberg

*Uppsala
2014*

Degree Project 30 credits within the Veterinary Medicine Programme

*ISSN 1652-8697
Examensarbete 2014:28*

Assessing the ability of LARGE overexpression to prevent the development of muscular dystrophy

Utvärdering av förmågan att förhindra utvecklingen av muskulär dystrofi genom överuttryck av LARGE

Astrid Rudberg

Supervisor: Professor Stina Ekman, Department of BVF

Assistant Supervisor: Professor Dominic Wells, Royal Veterinary College, London

Examiner: Leif Norrgren, Department of BVF

Degree Project in Veterinary Medicine

Credits: 30 hec

Level: Second cycle, A2E

Course code: EX0751

Place of publication: Uppsala

Year of publication: 2014

Number of part of series: Examensarbete 2014:28

ISSN: 1652-8697

Online publication: <http://stud.epsilon.slu.se>

Key words: Duchenne Muscular Dystrophy, muscular dystrophy, prevention, LARGE, mdx, mouse model

Nyckelord: Duchenne Muskulär Dystrofi, muskulär dystrofi, förhindra, LARGE, mdx, musmodell

Sveriges lantbruksuniversitet
Swedish University of Agricultural Sciences

Faculty of Veterinary Medicine and Animal Science
Department of BVF

SUMMARY

Duchenne Muscular Dystrophy (DMD) is a hereditary X-linked fatal disease that affects 1 in 3500 male births. It is the most common kind of muscular dystrophy in children and leads to death in the late teens or early 20s for many patients. The *mdx* mouse is a model of DMD that can be used to investigate experimental therapies. Overexpression of a glycosyltransferase, CT GalNAc, in *mdx* mice has been demonstrated to prevent the development of muscular dystrophy. Overexpression of another glycosyltransferase, LARGE, is currently being investigated as a treatment for another group of muscular dystrophies, the dystroglycanopathies.

In this study, we overexpressed LARGE in *mdx* mice in order to investigate its effect on the development of muscular dystrophy. We found that the transgene was expressed in our LV5/*mdx* mice, as seen with both immunohistochemistry and western blots, but that overexpressing the enzyme unfortunately appeared to have a negative effect on the dystrophy. An increase in pathology was seen histologically at both 3 and 8 weeks of age in the LV5/*mdx* mice when compared to the *mdx* mice. Physiological measurements on 22 week old mice showed a significantly diminished tolerance to eccentric exercise in the LV5/*mdx* compared to their *mdx* littermates. These observations lead us to the conclusion that increased expression of LARGE is not a therapeutic option for DMD patients, but is in fact contraindicated.

SAMMANFATTNING

Duchenne Muskulär Dystrofi (DMD) är en ärftlig X-linkad dödlig sjukdom som drabbar en av 3500 födda pojkar. Det är den vanligaste förekommande typen av muskulär dystrofi hos barn och leder till döden från sena tonår till tidig 20-års ålder för många av de drabbade. *mdx*-musen är en modell för DMD som kan användas för att utvärdera experimentella behandlingar. Överuttrycket av ett glykosyltransferas, CT GalNAc, hos *mdx*-musen har visat sig förhindra utvecklingen av muskulär dystrofi. Överuttrycket av ett annat glykosyltransferas, LARGE, undersöks just nu som en möjlig behandling för en annan grupp muskulära dystrofier, dystroglykanopatierna.

I den här studien har vi överuttryckt LARGE hos *mdx*-möss för att kunna undersöka dess effekt på utvecklingen av den muskulära dystrofin. Vi fann att transgenen uttrycktes hos våra LV5/*mdx*-möss med hjälp av både immunohistokemi och western blot, men att överuttrycket av enzymet tyvärr hade en negativ effekt på utvecklingen av dystrofin. En ökad nivå av patologi kunde ses på histologi gjord hos både 3 och 8 veckor gamla LV5/*mdx*-möss vid jämförelse med *mdx*-möss. Fysiologiska mätningar gjorda på 22 veckor gamla möss visade en signifikant minskad tolerans för excentrisk belastning hos LV5/*mdx* jämfört med deras *mdx* syskon från samma kull. Dessa iakttagelser fick oss att dra slutsatsen att ett ökat uttryck av LARGE hos DMD-patienter inte är ett alternativ för behandling, utan måste anses kontraindicerat.

TABLE OF CONTENTS

Abbreviations	1
INTRODUCTION AND LITERATURE REVIEW	2
Duchenne Muscular Dystrophy.....	2
<i>mdx</i> – a mouse model for DMD	3
LARGE as a possible treatment for MD	4
MATERIALS AND METHODS	4
Genotyping	4
Muscle Processing.....	5
Staining.....	5
Tiling	6
Western blot	6
Physiology.....	7
RESULTS.....	7
Generation of LV5/ <i>mdx</i> mice	7
Time point 8 weeks	8
Time point 3 weeks	11
IIF6 staining.....	12
Time point 20 weeks	13
Physiology.....	14
Western blot	15
DISCUSSION	15
Study limitations	18
Future work	19
CONCLUSION.....	19
ACKNOWLEDGMENTS.....	20
REFERENCES.....	21
APPENDIX.....	24

Abbreviations

α -DG – alpha-dystroglycan

β -DG – beta-dystroglycan

BMD – Becker Muscular Dystrophy

CMD – Congenital Muscular Dystrophy

CT GalNAc – Cytotoxic T cell GalNAc transferase

DAPs – Dystrophin associated proteins

DMD – Duchenne Muscular Dystrophy

DPM3 – DOL-P-Man synthase subunit 3

ECM – Extracellular matrix

FCMD – Fukuyama congenital muscular dystrophy

H&E – Haematoxylin and eosin staining

LGMD – Limb-Girdle Muscular Dystrophy

LV5 – mouse overexpressing LARGE

LV5/*mdx* – *mdx* mouse overexpressing LARGE

MD – muscular dystrophy

MEB – Muscle-eye-brain disease

POMGnT1 – Protein-O-mannose 1,2-Nacetylglucosaminyltransferase 1

POMT1 – Protein-O-mannosyl transferase 1

POMT2 – Protein-O-mannosyl transferase 2

TA – Tibialis Anterior

WT – wild type mouse

INTRODUCTION AND LITERATURE REVIEW

Muscular dystrophy (MD) is a group of hereditary diseases which are characterised by muscular weakness as a result of skeletal muscle wasting. There are many types of MD listed according to varying degrees of symptoms, location and age for onset of disease, such as Becker Muscular dystrophy (BMD), Duchenne Muscular dystrophy (DMD), Emery-Dreifuss muscular dystrophy, Congenital muscular dystrophy (CMD) and Limb-girdle muscular dystrophy (LGMD). Symptoms may start manifesting at birth or as late as in the 60s, and may include mental retardation (CMD) and cardiomyopathy (DMD, Emery-Dreifuss, LGMD) (Emery, 2002). The major cause of MDs is mutations in structural proteins such as dystrophin (DMD, BMD), sarcoglycans (forms of LGMD) or laminin (forms of CMD).

A new cause of MD has emerged during the last decade, with mutations in proteins that are putative or demonstrated glycosyltransferases causing a range of different clinical types of muscular dystrophy (Michele et al., 2002). The mutations result in a defective glycosylation of alpha dystroglycan (α -DG), leaving it hypoglycosylated. α -DG is a component of the dystrophin-glycoprotein complex present at the sarcolemma of skeletal muscle which undergoes glycosylation to regulate its ability to interact with extracellular matrix (ECM) proteins, changing between a hypoglycosylated and a hyperglycosylated state (Ervasti & Campbell, 1991). Mutations in seven genes coding for demonstrated or putative glycosyltransferases causing hypoglycosylation of α -DG have been identified so far: Protein-O-mannosyl transferase1 (POMT1; OMIM 607423; Beltran-Valero de et al., 2002), Protein-O-mannosyl transferase 2 (POMT2; OMIM 607439; van Reeuwijk et al., 2005), Protein-O-mannose 1,2- Nacetylglucosaminyltransferase1 (POMGnT1; OMIM 606822; Yoshida et al., 2001), Fukutin (OMIM 607440; Kobayashi et al., 1998), Fukutin-related protein (FKRP; OMIM 606596; Brockington et al., 2001), LARGE (OMIM 603590; Longman et al., 2003) and DOL-P-Man synthase subunit 3 (DPM3; OMIM 605951; Lefeber et al., 2009). Mutations in some of these are known to cause forms of CMD and LGMD, and they form part of the group of diseases caused by defective glycosylation of α -DG, now called dystroglycanopathies.

Duchenne Muscular Dystrophy

Duchenne Muscular Dystrophy (DMD) is the most common MD in children and was first described in 1851 (Meryon E, 1851). It is a fatal, X-linked recessive disease that affects approximately 1 in 3500 male births (Hoffman, 1987). The patients show delayed motor development and fail to meet motor milestones, such as starting walking and running, and patients often get diagnosed with the condition at a young age. The disease then progresses with increasing weakness, loss of ability to walk, scoliosis and in the late stages of the disease, cardiac and respiratory failure leading to death. Many patients die in their late teens or early 20s.

The disease is caused by mutations in the dystrophin gene, the largest gene on the X-chromosome. Different mutations have been associated with the disease, but they most commonly lead to a disruption of the open reading frame, which results in failure to translate

the mRNA into a functional protein. Patients suffering from this disease therefore have no dystrophin in their muscles, a structural protein normally located at the sarcolemma of the muscle fibres. This makes the muscle membrane fragile and prone to necrosis, leading to extensive damage. The tissue is progressively replaced by fibrosis and fatty connective tissue with time as the pool of satellite cells, the stem cells of skeletal muscles, is depleted (Cossu & Mavilio, 2000). BMD, which ranges from almost asymptomatic to close to DMD in clinical presentation, is associated with in frame mutations in the dystrophin gene, leading to a truncated protein. There is today no cure for either of these diseases, but some treatments, such as corticosteroids, can slow down the progression and give a better quality of life.

Approximately two-thirds of mothers of DMD patients are thought to be carriers of the defective gene, while the remaining cases represent new mutations occurring spontaneously in the dystrophin gene (Dubowitz, 1982). Of these carriers, approximately 8% show some kind of clinical symptoms. The female patients with manifesting disease show a symptom severity that inversely correlates with the proportion of the normal X-chromosome being expressed (via X inactivation), with a lower proportion giving more severe disease.

***mdx* – a mouse model for DMD**

As many other animal models, the mouse model for DMD was discovered by chance when screening was performed on mice for another experiment (Bulfield et al., 1984). It was later confirmed that this mouse indeed suffered from the same genetic disorder as the human patients, despite not showing the same clinical phenotype (Hoffman, 1987). It has a widespread use today in research for both DMD and BMD.

The *mdx* mice suffer from a mutation that occurred spontaneously in the dystrophin gene, creating a premature STOP codon located in exon 23 of the gene transcript. The translation of the dystrophin mRNA into protein is therefore made impossible, making the mouse dystrophin deficient. The absence of dystrophin makes the sarcolemma more fragile, resulting in increased necrosis of skeletal muscle fibres just as in the human patient.

There is an acute onset of pathology observed in the *mdx* mouse at around 3 weeks of age with massive muscle fibre necrosis and an increase in blood creatine kinase. This stimulates muscle regeneration in the areas of destruction, giving rise to patches of small, dystrophic myofibres with central nuclei. The nuclei will stay central for many months before a very small proportion of them become peripheral, making it easy to identify regenerated fibres at the histological level. The level of necrosis is stabilized by 8 weeks of age, staying on a relatively low level of active damage until the mouse reaches one year, when it is reduced even more. Differences in the pathology are seen depending on the muscle observed, e.g. with the diaphragm displaying more severe pathology than the muscles of the hind limb (Grounds et al., 2008).

The pathology observed in the mouse model is much less severe than in humans suffering from the disease. This may be due to the difference in weight and in load on the muscles, but also the difference in the locomotor apparatus, comparing a biped to a quadruped (Grounds et

al., 2008). The mild phenotype observed in the *mdx* mouse may also mean that the pool of satellite cells lasts its whole lifetime, resulting in less extensive fibrosis compared to humans (Cossu & Mavilio, 2000).

LARGE as a possible treatment for MD

Mutations in the putative glycosyltransferase LARGE is one of the seven causes of dystroglycanopathy reported so far. It is a protein ubiquitously expressed in the body that is mainly confined in the Golgi apparatus within the cell (Brockington et al., 2005). Viral gene transfer into cell cultures derived from patients suffering from dystroglycanopathies suggests that this particular enzyme can functionally compensate for other glycosylation defects (Barresi et al., 2004) and later, this was also demonstrated *in vivo* in a mouse model (Kangawa et al., 2009). Seeing as only very few cases of patients with mutations in LARGE has been reported worldwide (Mutoni et al., 2008), this discovery displays a very big therapeutic potential for the dystroglycanopathies. In addition, Nguyen et al (2002) and Martin et al (2009) discovered that the overexpression of CT GalNAc, another glycosyltransferase localized in the neuromuscular synapses in adult skeletal muscles, prevents MD development in *mdx* mice when looking at both the histology and physiology.

Following these publications, a mouse overexpressing LARGE was generated by Brockington et al (2010), showing no histological pathology in any muscles. This now opens up the possibility of assessing the potential for upregulation of LARGE expression as a therapy for a range of muscular dystrophies by crossing this transgenic with the different mouse models of muscular dystrophy.

This investigation has been aimed at assessing if the overexpression of LARGE in *mdx* mice can prevent the development of MD, by looking at different time points and using different techniques for assessing histopathology and physiology.

MATERIALS AND METHODS

Genotyping

Mice overexpressing LARGE were generated as described in Brockington et al (2010). These were crossed with *mdx* mice, and the offspring were genotyped by using PCR to identify the transgenic individuals. Ear biopsies taken after weaning were put in 100 µl ear buffer (originating from a 10x stock solution consisting of 500 mM KCl; 100 mM Tris-HCl pH 8,3; 0,1 mg/ml Gelatin; 0,45% v/v Tween 20; 0,45% v/v Nonidet P40; 5 mg/ml Proteinase K) and left overnight in a 50°C water bath to digest the proteins and liberate the DNA. The following day, they were heated in a block at 100°C for 10 minutes to degrade the proteinase K used to digest the biopsy.

A master mix was made up based on the basic recipe of 17 µl of double distilled water, 2,5 µl of buffer, 2,5 µl enhancer solution, 0,5 µl of MgCl (50 mM), 0,75 µl of dNTP (2,5 mM/nucleotide), 0,5 µl of forward (T7; TAATACGACTCACTATAGG) and reverse (LGS1; CTGCCCAATGCTAAGATG) primers (10 pM/µl) and 0,25 µl Taq polymerase. This made

up 24,5 µl of master mix that was mixed with 0,5 µl of sample that was then run in the PCR with the running conditions of 5 minutes at 94°C for initial denaturation, then 35 cycles of 15 seconds at 94°C, 30 seconds at 55°C and 30 seconds at 68°C, followed by a 10 minutes final extension at 68°C.

6 µl of loading buffer (Ficoll and bromophenol blue) was added to each sample before they were run in a 1% agarose gel (1 g agarose powder mixed with 100 ml TBE Trisboric acid EDTA) where SYBR safe (5 µl/100 ml gel) had been added. The gel was run at 70 V for 40 min, and a 1 kb ladder was used. The results were visualized in a UV-box.

Muscle Processing

The samples collected from the mice for histology and western blots were quadriceps, diaphragms, soleus, Extensor Digitorum Longus (EDL) and Anterior Tibialis (AT). The mice were killed by cervical dislocation and the muscles dissected and mounted on pieces of cork with OCT and then snap frozen in isopentane that was cooled in liquid nitrogen. The samples were wrapped in foil and kept in a -80°C freezer. When using them for cryosectioning, the samples were transported on dry ice to the cryostat and left for 30 minutes to equilibrate to -20°C. Sections were cut at 10 µm and placed on Superfrost slides. Approximately 8-12 different levels within the muscle were collected onto the same slide and ten serial slides were generated. The number of sections discarded between each level in the muscle varied depending on tissue and age (8 week quadriceps: 40 discards, 8 week diaphragms: 25 discards, 3 week quadriceps: 10 discards, 3 weeks diaphragm: 10 discards, 20 weeks diaphragm: 30 discards). The slides were left out to dry for 10 minutes before they were stored in a -80°C freezer.

Staining

Harris's haematoxylin (ratio 1:1 with water) and 1% eosin was used for the H&E staining. The slides were left to air-dry for 20 minutes after removal from the -80°C freezer and then left for three minutes in the haematoxylin. They were then placed in running water for four minutes, followed by 40 seconds in eosin, after which the slides were briefly washed in water. The slides were then progressively dehydrated in alcohol (70%, 80%, 90% and 100%) and then cleared for 20 minutes, followed by another 60 minutes in xylene. DPX was used to mount the cover slip, and the finished slides were left to dry in the fume hood until the next day. Colour images were taken with the Bright Field upright DM4000B using the Leica Application Suite software.

Immunohistochemistry was done on the 8 week and 3 week quadriceps using the I1H6 antibodies. This binds to glycosylated epitopes, which in this case is primarily the hyperglycosylated α -DG. As before, the slides were allowed to air-dry for 20 minutes and then left to incubate overnight in 1:200 I1H6 at 4 °C. The following day, they were washed (3 times for 3-5 minutes) in PBS and then left to incubate in 1:200 biotinylated polyclonal rabbit anti-mouse Ig M for 30 minutes. The slides were washed again and then incubated in 1:1000 Streptavidin and 1:2000 Hoechst for 20 minutes before being washed and then mounted with

hydramount. They were visualized in the Fluorescent upright DM4000B microscope and pictures were taken using the Zeiss AxioVision software.

Alizarin red S staining for calcium was done to confirm the presence of calcium deposits in the muscles of the 8 week old mice. Sections were taken from the -80°C freezer and left to dry for a few minutes before they were fixed in cold acetone for 10 minutes. They were then left to dry again before they were rinsed in distilled water. The slides were immersed in Alizarin red solution (Alizarin red S: 2g; Distilled water: 100 ml; pH: 4,2) for 1 minute. The slides were then blotted dry, before being rinsed in acetone for 30 seconds and then rinsed in acetone/xylene (1:1) for 15 seconds, and finally cleared in xylene for 20 minutes followed by another 60 minutes before they were mounted with DPX. Imaging was performed as with the H&E stains.

Tiling

In order to perform various image analyses, tiling was done with the H&E slides. This creates a high contrast, black and white image of the slides using a merged image of several small pictures. The Leica SP5 confocal microscope with the Leica Application Suite Advanced Fluorescence software was used to do this. These images were then used to perform counts on total number of fibres and number of non-centrally nucleated cells with the help of Photo Shop and Image J. The definition set for a non-centrally nucleated cell was any muscle fibre that had nuclei that were in contact with the membrane, or were not further away from the membrane than the diameter of a nucleus. Any fibre that had no visible nucleus in the section, but had a clearly darker colour than the surrounding fibres, was regarded as a regenerating fibre and therefore not counted as a non-centrally nucleated fibre. The area counted was limited to the rectus femoris as this muscle was well limited and undamaged in most of the sections. Three counts of total number of fibres were done per group (n=3) and averages were based on these. The counts of non-centrally nucleated fibres were done blinded to sample identity.

Western blot

Protein extraction was performed in a sample buffer consisting of Tris HCl 75 mM, pH 6,8; SDS 1% and a protease inhibitors (Complete, Mini; Protease Inhibitor Cocktail Tablets, Roche according to manufacturer's instructions). The muscles were first weighed, and then crushed with a pestle and mortar that had been cooled down with liquid nitrogen. The powdered muscle was collected in eppendorfs and sample buffer added (2µl/ mg tissue). The samples were then heated (3 minutes in 100 °C) and then centrifuged (10 minutes at 14 000 g at 4 °C).The supernatant was transferred into new eppendorfs. The samples were then stored on dry ice until a protein quantification assay was performed on them. Quantification of the total protein in each sample was performed using the DC Protein Assay (BIORAD) on samples than had been diluted 1:20 with filtered water. Standards were made up according to instructions in the Comassie Plus Protein Assay Reagent kit. After quantification the samples were aliquoted and stored at – 80°C.

Polyacrylamide gel electrophoresis was performed in a XCell *SureLock*TM Mini-Cell (Invitrogen) using precast NuPage Novex Bis Tris 4-12% gradient gels according to manufacturer's instructions. 20 µl total volume was loaded per well, consisting of 20 µg of total protein, 1 µl of NuPage Sample Reducing Agent (10x), 5 µl of NuPage 4X LDS Sample Buffer and RO water. Electrophoresis was performed in NuPage 1 X MOPS SDS Running Buffer with 0.5 ml of NuPage Antioxidant. The gel was run at 200 V for 90 minutes.

Transfer of the proteins to a nitrocellulose membrane (HybondC – GE Healthcare) was performed in an XCell IITM Blot Module (Invitrogen) according to manufacturer's instruction, in 1 X NuPage Transfer Buffer at 30V for 2h 30 minutes. After transfer the membrane was transferred into blocking solution, 3% BSA (Jackson ImmunoResearch) in IHH6 blocking buffer (100 mM NaCl; 20 mM Tris pH 7.4) overnight at 4C.

Immunostaining was performed with monoclonal antibody IHH6 (1:2500) or polyclonal Rabbit anti- β -tubulin antibody diluted in IHH6 blocking buffer with 3% BSA for 1 h on the roller mixer at room temperature. The membrane was washed thoroughly (3 X 10 minutes in IHH6 blotting buffer) before incubation with the secondary antibodies, either polyclonal rabbit anti-mouse IgM biotinylated antibody (1:2000) for IHH6 or anti-rabbit Ig G HRP conjugate for β -tubulin (1:5000). Secondary antibodies were diluted in IHH6 blotting buffer and incubated for 1 h at room temperature. The membrane was washed (3 x 10 minutes in IHH6 blotting buffer). For IHH6 staining a further round of signal amplification was performed with Streptavidin-HRP conjugate (1:10 000) diluted in IHH6 Blotting Buffer incubated for 1hour at room temperature. The membrane was washed again in IHH6 blotting buffer. Antibodies were visualised using an ECL plus chemiluminescence detection system (GE Healthcare, according to manufacturer's instructions). The membranes were exposed to x-ray films in a dark room to obtain the clearest result.

Physiology

Physiology was performed on both groups of mice at 22 weeks of age, using methods described in Brockington et al (2010). The distal tendon of the TA of anaesthetised mice was dissected from surrounding tissue and attached to a servomotor transducer in order to record several physiological measurements, such as the peak twitch force, maximum isometric tetanic force and the susceptibility of the TA muscle to eccentric contraction-induced injury. This was done while carefully monitoring the mouse and using previously tested protocols for the different measurements.

RESULTS

Generation of LV5/*mdx* mice

Male mice overexpressing LARGE (described in Brockington et al., 2010) were crossed with female *mdx* mice, generating offspring where in theory 50% of the pups should be carrying the LARGE gene and all the male mice were *mdx* as the *mdx* allele is on the X chromosome. The pups were genotyped using PCR, and then separated into one experimental group (LV5/*mdx*) and a control group (*mdx*) with littermates present in both groups (Figure 1). In

subsequent generations LV5/*mdx* male mice were crossed with *mdx* females so that both sexes could be used.

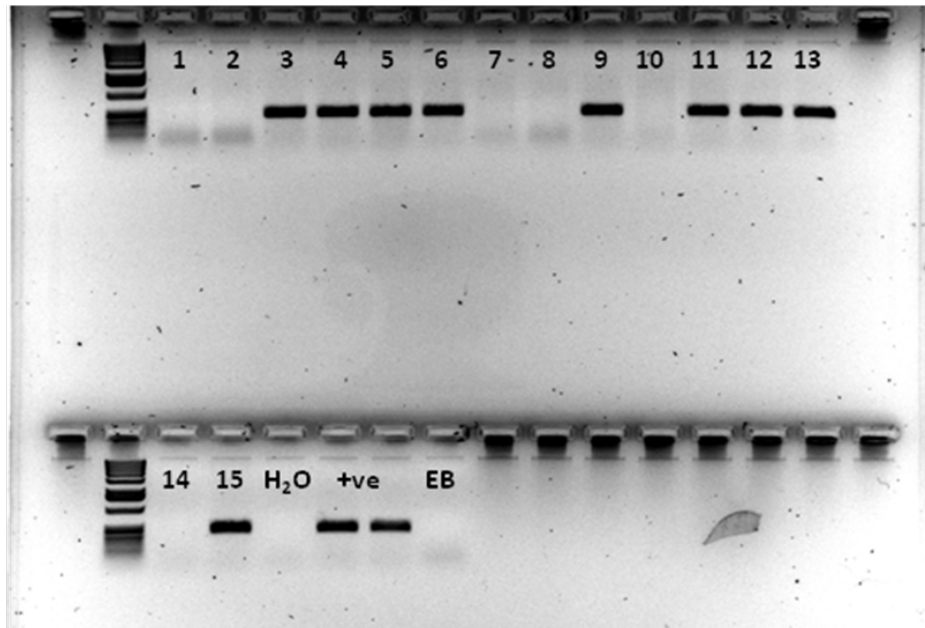


Figure 1. Genotyping offspring of LV5 and *mdx* mice. 15 ear samples followed by water (negative control), two known LV5 positive controls and ear buffer (EB, negative control). Positive samples in wells 3, 4, 5, 6, 9, 11, 12, 13 and 15.

Time point 8 weeks

The first time point we chose for comparison was 8 weeks. At that point, the level of necrosis in the *mdx* model should have stabilized to a relatively low level and fibres in all stages could be seen in the muscle. We started off looking at quadriceps from the two groups.

When examining the blinded H&E slides from 8 week quadriceps (n= 6 per genotype, all males), deposits of some kind were found in almost all of the samples. There was a varying degree of destruction and inflammation seen in the tissue, but some differences were observed that made it possible to separate the mice into two groups (figure 2). Differences in the number of fibres with centralized nuclei, and in the morphology of the fibres were observed. One group, which was found to be the LV5/*mdx*, appeared to have almost 100% fibres with centralized nuclei, whereas the other group, *mdx*, had a more visible proportion of fibres with non-centrally nucleated fibres. This observation was confirmed when counting of the fibres was done on tiled images (figure 3), showing a clear significant difference ($p < 0.0001$) between the two groups when performing an unpaired t-test with the percentage of non-centrally nucleated fibres (figure 4). The LV5/*mdx* also appeared to be more heterogeneous in fibre size than the *mdx*. They displayed groupings of very small regenerating fibres, and groups of big fibres.

We proceeded to look at the diaphragms of the same individuals (n=6 per genotype, all males). As expected, the pathology in this tissue was more severe than that observed in the

quadriceps as it is a muscle that is in constant use. The deposits found in the quadriceps were also found in the diaphragms when looking at the slides after H&E staining, but they were present in larger quantities. As they were suspected to be calcium deposits, alizarin red staining was performed. This stains the calcium present in the sample intensely red and makes it easily distinguishable from the rest of the tissue. The suspicion about calcium was confirmed as the deposits stained very intensely (figure 5). There was also a clear difference observed between the two groups, with the LV5/*mdx* showing a bigger quantity of deposits located throughout the diaphragm. The *mdx* had a smaller quantity of deposits that was frequently located in one area.

The findings made at this time point indicated a more severe pathology in the LV5/*mdx* mice compared to the *mdx*. The decision to look at an earlier time point was made, in order to investigate whether the pathology in the LV5/*mdx* started earlier than in the *mdx*, or if it had the same starting point but with a more intense pathological development.

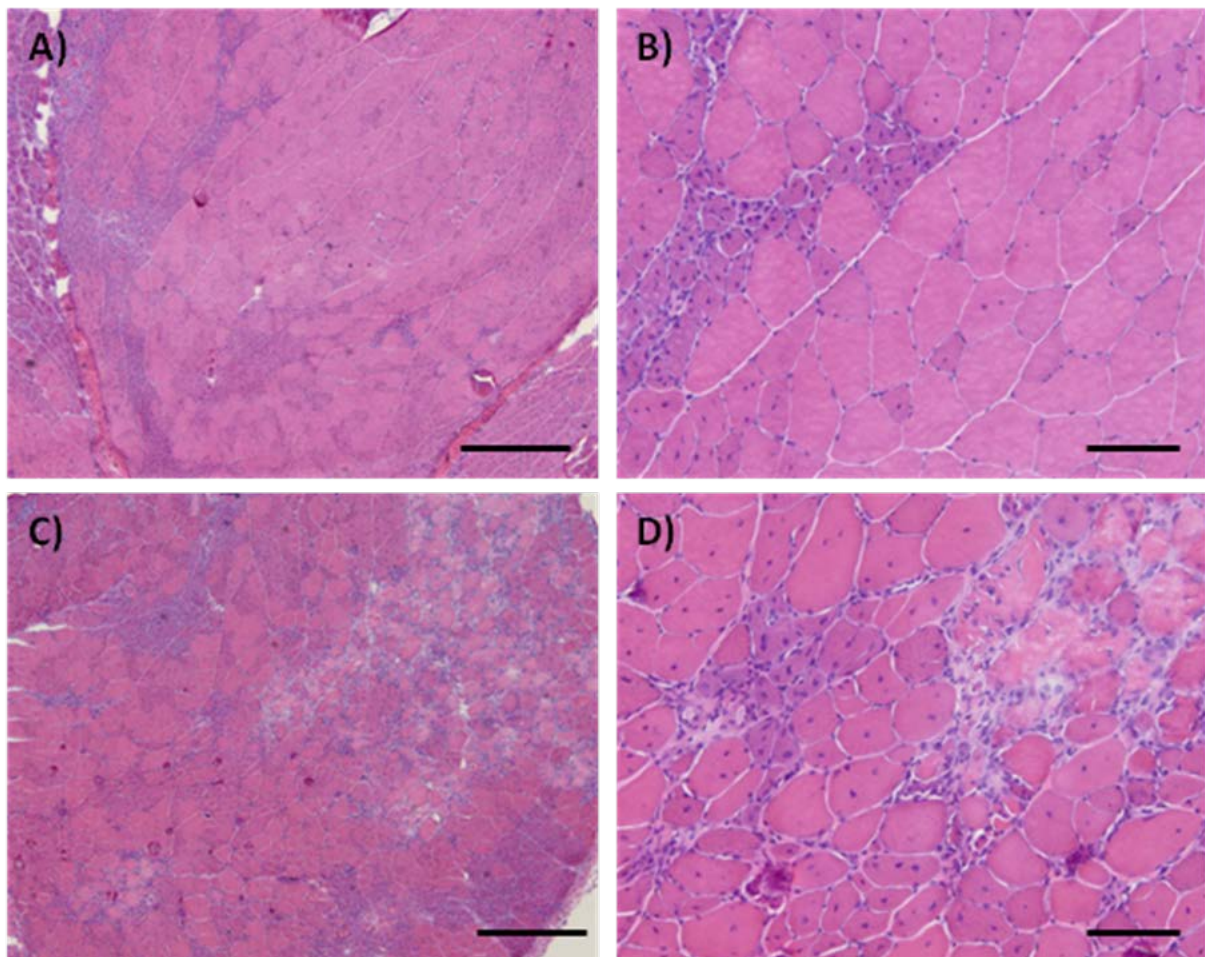


Figure 2. Rectus femoris muscle in 8 week old *mdx* and LV5/*mdx* mice. H&E staining of transverse cryosections of quadriceps from *mdx* (A and B) and LV5/*mdx* (C and D) mice. More centralized myonuclei can be seen in the LV5/*mdx* mouse compared to the *mdx* mouse. Scale bar 500 μm in A and C, and 100 μm in B and D.



Figure 3. Tiling of images to show the complete rectus femoris on a LV5/*mdx* mouse.

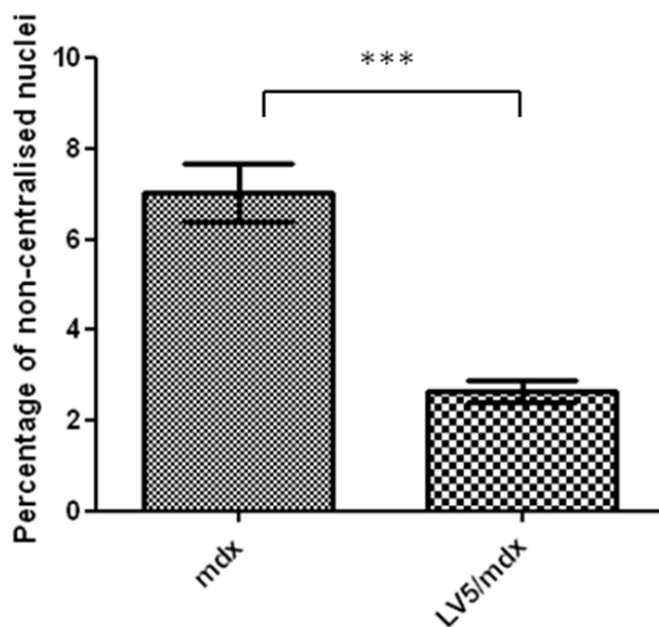


Figure 4. Percentage of non-centralised myonuclei in 8 week old *mdx* and LV5/*mdx* mice. Results are expressed as mean \pm standard deviation of percentage non-centralised myonuclei in relation to total number of fibres in the rectus femoris (n=6 per group). The number of non-centralised myonuclei is significantly higher in the *mdx* compared to the LV5/*mdx*. *** $p < 0,0001$ for comparison between *mdx* and LV5/*mdx* with unpaired t-test.

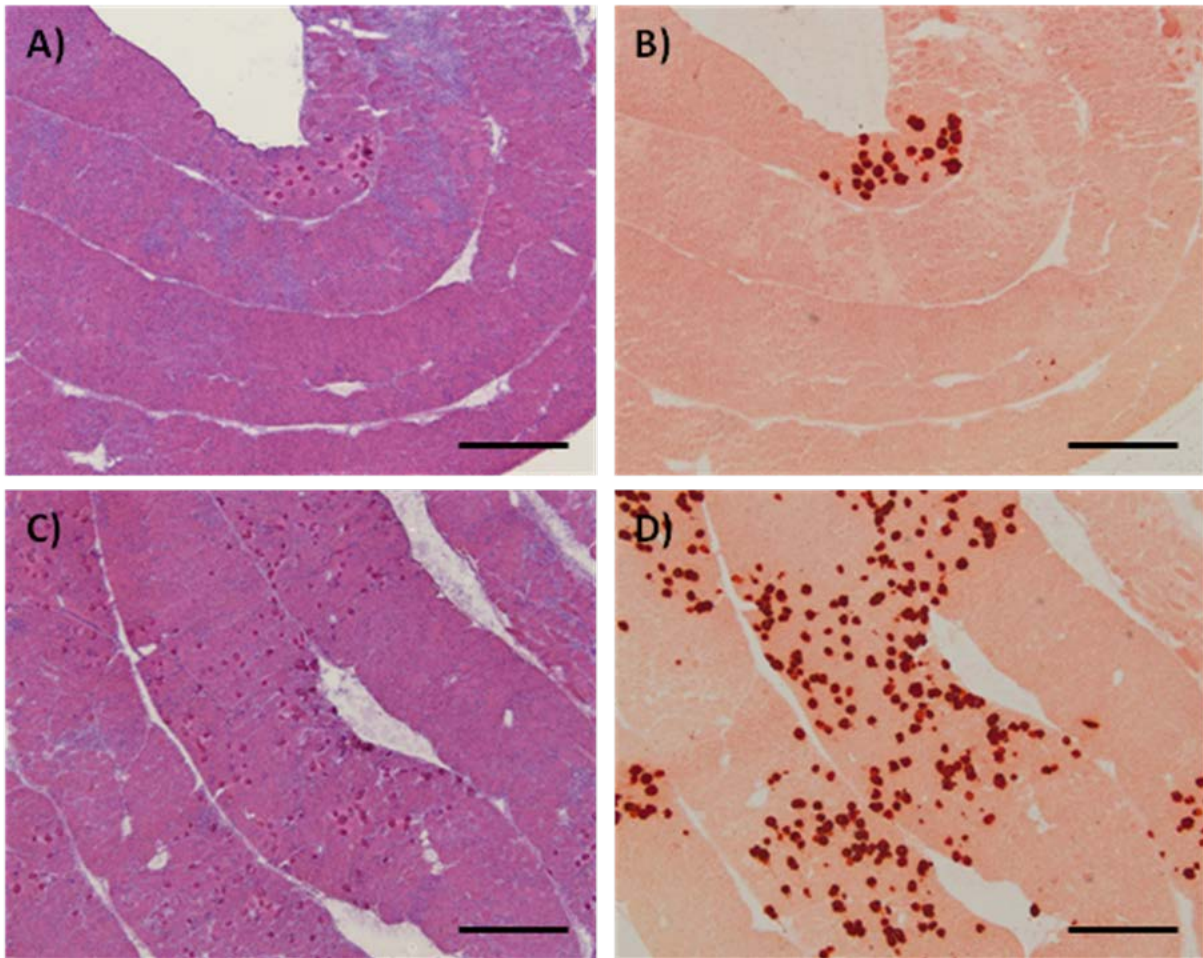


Figure 5. Diaphragm in 8 week old *mdx* and LV5/*mdx* mice. Transverse frozen sections of diaphragm in *mdx* (A and B) and LV5/*mdx* mice (C and D). H&E staining (A and C) and alizarin red staining (B and D). The presence of more calcium deposits in a larger area is seen in the LV5/*mdx* compared to the *mdx*. Scale bar-500 μ m.

Time point 3 weeks

The pathology in the *mdx* mice is said to start at 3 weeks of age (Grounds, 2008). We therefore decided to take this as the next time point for investigation. The mice chosen were 20 days old and originated from three litters.

When looking at the samples blinded, the quadriceps could be grouped into two groups (n=5; LV5/*mdx*: 1 female, 4 males; *mdx*: 1 male, 4 females) based on the degree of destruction and inflammation. The LV5/*mdx* showed a much higher degree of destruction and inflammation than the *mdx* (figure 6). The destruction was seen in various places in the quadriceps muscle, sometimes being only apparent in the rectus femoris and not at all in the vastus muscles (musculus vastus medialis, lateralis et intermedius), other times completely the opposite. No apparent pattern of destruction could be determined.

The diaphragms of the same individuals (n=5) were examined, but no clear difference could be observed.

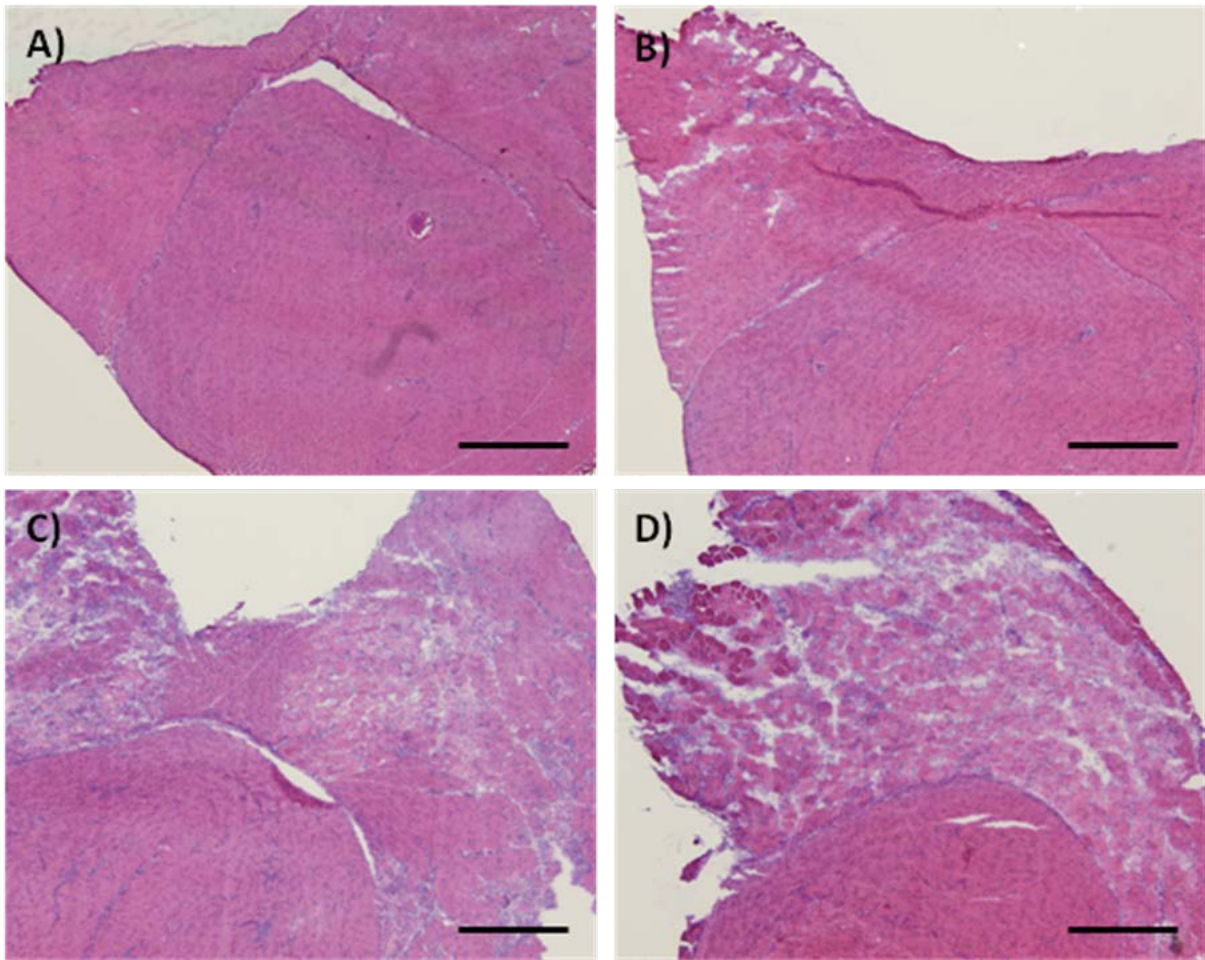


Figure 6. Quadriceps muscle in 3 week old *mdx* and *LV5/mdx* mice. Transverse frozen sections of quadriceps in *mdx* (A and B) and *LV5/mdx* (C and D) mice. H&E staining. The individuals with the least amount of damage within their group (A and C) and the individuals with the greatest amount of damage (B and D). The overall level of damage observed is much greater in the *LV5/mdx* mice compared to the *mdx* mice. Scale bar- 500 μ m.

IIIH6 staining

The IIIH6 staining was done on sections of quadriceps from the 3 and 8 week mice in order to confirm the overexpression of LARGE in the muscle. Confirmation was obtained in all the 8 week samples, as a clear difference could be seen between the two groups when viewed blinded (figure 7). The IIIH6 was seen bound in much greater quantities in the sections originating from *LV5/mdx* mice, displaying a clear outline of the individual muscle fibres. A similar difference was observed when looking at the 3 week quadriceps.

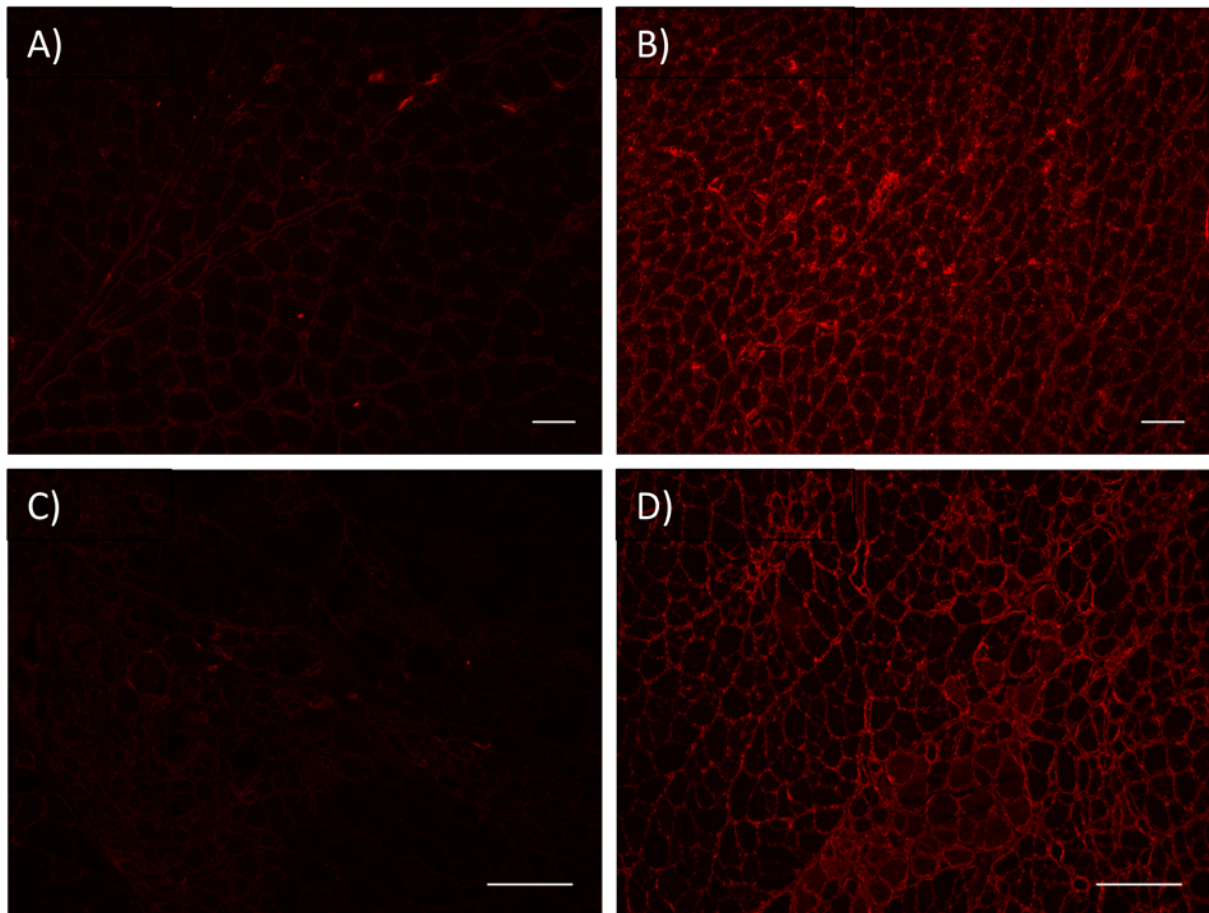


Figure 7. Immunohistochemistry of *mdx* and *LV5/mdx* mice quadriceps. Transverse frozen sections of quadriceps from *mdx* (A and C) and *LV5/mdx* (B and D) mice aged 3 weeks (A and B) and 8 weeks (C and D) stained with I1H6 antibodies. The *LV5/mdx* individuals show a much more intense staining compared to the *mdx*, confirming the expression of the LARGE transgene. Scale bar-100 μ m.

Time point 20 weeks

With the difference seen between the two groups at an early stage, the question whether a difference could be observed at a later stage as well arose. A small number of mice aged 20 weeks were selected to have a preliminary look (*LV5/mdx*, n=2; *mdx*, n=1; all males). The difference most likely to be seen at this stage was in the development of fibrosis, and therefore the diaphragm was examined. When the H&E slides were viewed blinded, there was a clear development of fibrosis observed. Deposits were present in large quantities, and many hypertrophied fibres were seen (figure 8). No clear difference could be established between the two groups.

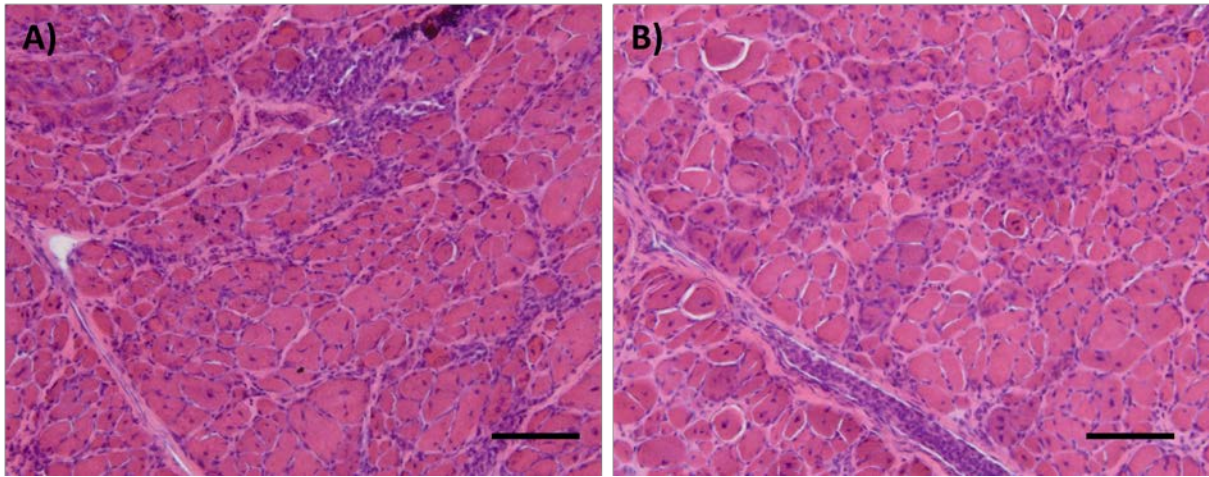


Figure 8. Diaphragm of a 20 week old *mdx* and *LV5/mdx* mouse. Transverse frozen sections of diaphragm from *mdx* (A) and *LV5/mdx* (B) mice at 20 weeks. No difference between the two groups could be established. Scale bar-200 μ m.

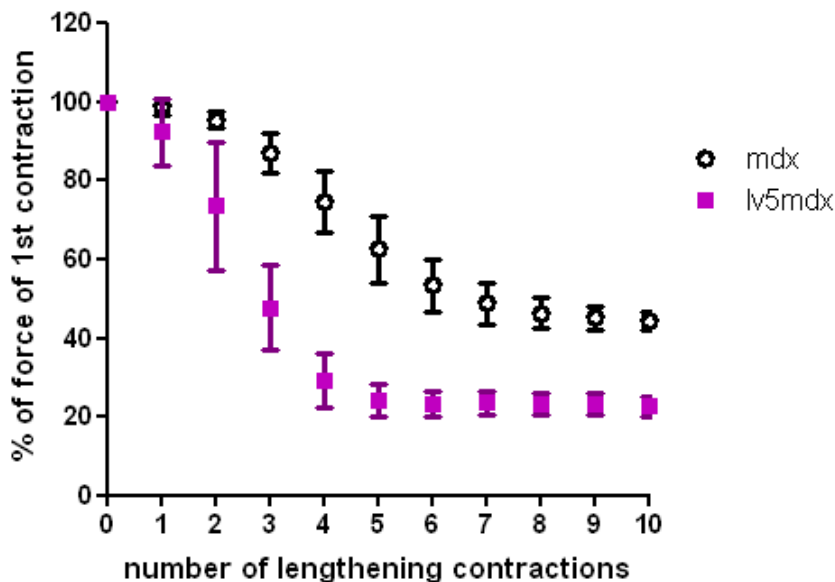


Figure 9. *In vivo* response to lengthening contraction. Percentage of force drop during eccentric exercise protocol with a 15% stretch of the TA in 22 week old mice (n=3 per group). Results are expressed as mean \pm standard error of mean. The *LV5/mdx* mice showed significantly greater force drop compared to the *mdx* littermates with increasing number of contractions (p=0,0086 between the two curves).

Physiology

As there was no clear difference seen between the two groups histologically in the diaphragm in the older mice, we investigated if there was a physiological difference. Physiological measurements was done by Rebecca Terry on 22 week old mice (n=3 for both genotypes, all males) as previously described (Brockington et al., 2010). The eccentric exercise protocol showed a clear significant difference (p=0,0086 with repeated measures ANOVA) between

the two groups, with one displaying an earlier and more rapid decrease in force than the other. The LV5/*mdx* group showed a much decreased tolerance to the contractions compared to the *mdx* as the decrease in force observed indicates muscle damage (Figure 9).

Western blot

We used paired samples for both groups at 3 and 8 weeks of age (n=2 per group, all males) as well as a WT and a LV5 (n=1, male) (figure 10). The blot showed the normal glycosylation in the WT and the expected hyperglycosylation in the LV5. The 3 week *mdx* showed almost no glycosylation, whereas the 8 week *mdx* showed a limited level. The LV5/*mdx* displayed a clear hyperglycosylation at both time points, which confirms the presence and expression of the LARGE transgene in these animals. Similar results were obtained for another 3 samples from 8 week mice (n=3 per group, all males) in western blots performed by Dr Mark Ackroyd.

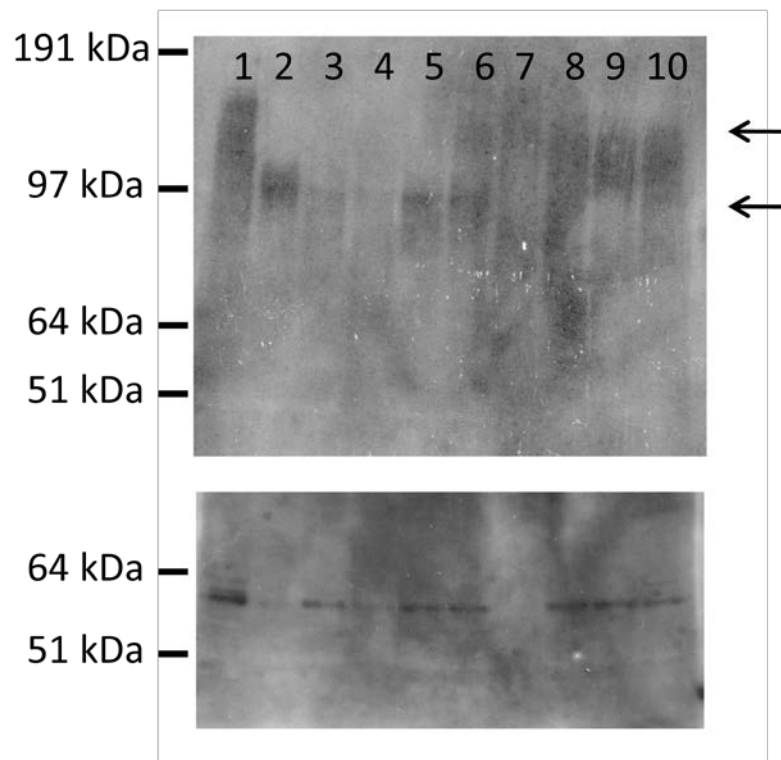


Figure 10. Western blot of mouse muscle. Western blot analysis of protein lysates with IIH6 antibodies against α -DG. Quadriceps muscle from LV5 (lane 1), WT (2), 3 week *mdx* (3 and 4), 8 week *mdx* (5 and 6), 3 week LV5/*mdx* (7 and 8), 8 week LV5/*mdx* (9 and 10). Hyperglycosylation can be seen in lane 1, 7, 8, 9 and 10. Upper arrow shows hyperglycosylation while the lower arrow shows normal glycosylation.

DISCUSSION

Overexpression of LARGE represents one of the many strategies being pursued to find a treatment for DMD and other MDs. It has been demonstrated that overexpression of LARGE increases the glycosylation of α -DG (Brockington et al., 2005), which is the process that is

defective in dystroglycanopathies. If proven successful, the LARGE initiative has the potential for treating a number of MDs, especially since even partial restoration of α -DG glycosylation can ameliorate the progression of the diseases noticeably (Kanagawa et al., 2008).

Unfortunately, this study reveals that LARGE is not alternative therapeutic option for DMD patients. At 3 weeks, the LV5/*mdx* mice show a more severe pathology with an earlier onset compared to the *mdx* mice. This is once again seen at 8 weeks when the LV5/*mdx* mice had more advanced pathology as indicated by the significantly reduced count of non-centrally nucleated fibre compared to the *mdx*, resulting from a higher rate of fibre necrosis. The greater amount of calcium deposits found in the diaphragms of the LV5/*mdx* compared to the *mdx* indicates once again a higher level of damage in the muscles of the transgenic group. When performing physiology on 22 week old mice, the eccentric exercise protocol reveals a much higher susceptibility to fibre damage in the LV5/*mdx*, showing that the membranes of the muscle fibres are much frailer in the LV5/*mdx* than in the *mdx*.

In the case of the *mdx* mice, the increased glycosylation of α -DG seem to have a detrimental effect on the viability of the muscle fibres. More pathology is observed histologically, and a clear negative effect is seen on the physiology. The increased glycosylation most likely increases the attachment of the sarcolemma to the ECM proteins, such as perlecan, agrin and laminin. It seems as though the increased attachment to the ECM, in the absence of dystrophin to transfer the force to the internal cytoskeleton, decreases the fibre stability.

There is also the possibility that overexpression of LARGE does not only lead to hyperglycosylation of α -DG, but to other components of the sarcolemma as well. This might also lead to an increased attachment to the ECM, but of another kind. If this is the case, the missing dystrophin may not be the problem, which subsequently means that treatment with upregulation of LARGE may prove to be unsuccessful in models for dystroglycanopathies as well. The study done on the LV5 transgenic mice did not reveal any histological pathology in any muscles, but there was an increased susceptibility to contraction-induced injury in the older mice (8 months old) (Brockington et al., 2010). The *mdx* background of our mice, giving them decreased muscle fibre viability to start with, may highlight and increase what was starting to show in the 8 month LV5 mice.

DMD patients and the *mdx* mice do not have a problem in the glycosylation of α -DG to begin with, but yet the overexpression of another glycosyltransferase in the *mdx* decreases the pathology significantly in *mdx* mice (Nguyen et al., 2002; Martin et al., 2009). It has been shown that the loss of dystrophin in both DMD patients (Ohlendieck et al., 1993) and the *mdx* mouse (Ohlendieck & Campbell, 1991) reduces the expression of many dystrophin-associated proteins (DAPs) that are in the proximity or directly bound to dystrophin. These include the dystroglycans, dystrobrevins and sarcoglycans. In the case of the CT GalNAc transferase, the overexpression of this enzyme leads to restoration of normal or above normal expression of the DAPs (Nguyen et al., 2002) which seems to be the factor preventing the muscular dystrophy. LARGE only increases glycosylation, but with the decrease in α -DG and the other

DAPs observed in the *mdx*, one can wonder what other molecules on the membrane actually get glycosylated. Interestingly, a newly published paper by Zhang et al. (2011) showed that overexpressing LARGE in α -DG deficient neural stem cells still gave binding of IIIH6 antibodies, when it has been thought that they only bind to hyperglycosylated α -DG. This not only questions the specificity of the IIIH6 immunoreactivity, but also confirms that LARGE glycosylates at least one other molecule on the cell surface. The glycosylated molecules were also shown to possess the functional capacity of binding laminin.

The presence of calcium aggregations in DMD patient biopsies has been reported for a long time (Bodensteiner & Engel, 1987), and the same is reported for *mdx* mice (Turner et al., 1991). This is the result of a higher intracellular calcium level present in the dystrophic muscle fibres. There are two theories to why this is the case; one speculates that it is the result of tears in the debilitated membrane during eccentric contractions, the other that it is caused by abnormal functioning of membrane channels, mainly stretch-activated channels (Whitehead et al., 2006). Both of these lead to an increase in intracellular calcium, which means the loss of calcium homeostasis within the fibre. This subsequently triggers various pathways, such as proteases and reactive oxygen species, leading to fibre necrosis. In the case of the LV5/*mdx*, the greater presence of calcium deposits in the diaphragm at 8 weeks bears witness of an increase in the destructive process of calcium infiltration. The increased attachment between the sarcolemma and the ECM, leading to increased tearing of the membrane during eccentric exercise, would be a possible hypothesis for this finding.

The reason for the acute onset of pathology at 3 week of age in *mdx* mice is not known, but one hypothesis is that it is caused by an increase in activity of the pups as that is generally when they start exploring the cage, or it could be the result of a developmental change in protein expression in the mouse (Grounds et al., 2008). In any case, it provides a good time point for comparison when evaluating potential therapies targeting a reduction of necrosis, which is demonstrated quite clearly here. The fact that no difference could be seen between the diaphragms of the two groups at 20 week may be an indication of that the pathology in the *mdx* has caught up to the one in the LV5/*mdx*, explaining why they both show similar levels of fibrosis and hypertrophy of the muscle fibres.

LARGE has previously been overexpressed experimentally through viral vector transfer in the Large^{myd} mouse, a mouse with a spontaneous mutation in LARGE (Barresi et al., 2004). It serves as a mouse model for dystroglycanopathies such as muscle-eye-brain disease (MEB) and Fukuyama congenital muscular dystrophy (FCMD). The overexpression of LARGE resulted in an improved phenotype in the Large^{myd} mouse, decreasing the pathology. An even more promising result was found when the overexpression of LARGE in the knock-in mouse model for FCMD and in the POMGnT1 mouse model (Kanagawa et al., 2008) lead to the production of α -DG capable of binding laminin in both cases, although nothing is said about the phenotype. These are promising results for LARGE, but more research needs to be done using animal models for dystroglycanopathies, such as the Sox1FKRP^{KD} (Brown et al., in preparation).

The increase in glycosylation level seen between the 3 and the 8 week old mice on the western blot can be attributed to an actual increase of DAPs. It has been shown that neonatal muscle and regenerating patches in *mdx* mouse muscles have a much higher expression of DAPs compared to mature muscle in *mdx* (Khurana et al., 1991). As there is a large presence of regenerating patches at 8 weeks, the glycosylation level becomes visible on western blot.

Study limitations

The counting done on total number of fibres in the 8 week individuals (appendix 1) shows that there was an outlier in the LV5/*mdx* group. We discussed excluding it, but found that this would only create a bias in favour of more pathology in the LV5/*mdx*. The larger number of fibres seen in the LV5/*mdx* group is thought to be due to fibre splitting due to defects in regeneration and is commonly seen in older *mdx* mice (Lovering et al., 2009).

The 3 week old mice is the only time point where females are present. They were the second generation of the LV5/*mdx* cross, which meant that both sexes could be used. Unfortunately, the sex ratio between the two groups turned out to be very marked, which is an important factor that needs to be taken into account when considering the results. It has been shown that gender plays a role in the pathology observed in the *mdx*, with females showing a lower susceptibility to muscle damage at a young age compared to males, but a higher level of fibrosis when old (Salimena et al., 2004). The 3 week old mouse displaying the severest pathology in the *mdx* group turned out to be the male, and the mouse showing the least pathology in the LV5/*mdx* was the female. This indicates the need of increasing the n number and balancing out the sexes between the two genotypes before final conclusions to be made.

The IIF6 staining on the 3 week mice worked, but was patchy. The presence of more intensely stained neuromuscular junctions in the *mdx* sections made it possible to identify when it had worked on an *mdx* sample. This experiment could not be repeated again because of time constraints but should be repeated before publication of this study.

There is some question as to whether the statistical test done for the physiological measurement can be used with such low n numbers. The study was repeated with another two mice in each group and showed the same pattern, but with different values, which was most likely caused by the use of different equipment. This again needs to be repeated before the publication of this study.

The WB image shows that there was some problems with the loading control as a few bands appear faint or missing. With regards to the LV5/*mdx* and the *mdx* samples, these were run in pairs and at least one of the loading controls for them worked properly. This validates the experiment. Additional samples run by Dr Mark Ackroyd on 8 week mice (n=3) displayed similar results (figure not included) which validates this further. There is also evident background coming through in the picture caused by non-specific binding by the antibodies, but again because of time constraints, the experiment could not be repeated.

The overexpression of the CT GalNAc transferase protected against muscular dystrophy, while overexpression of LARGE did not. In the CT GalNAc transferase experiment, protection was associated with restoration of the DAPs. The level of the DAPs in the LV5/*mdx* in comparison to the *mdx* needs to be investigated.

Future work

As well as the experiments noted above to complete the *mdx*/LV5 study, more research needs to be done in the area of LARGE overexpression, mainly with generation and analysis of animal models for dystroglycanopathies overexpressing LARGE. The Wells/Brown groups plan to examine the effects of overexpressing LARGE in Large^{myd} mice, Sox1FKRP^{KD} mice and POMGnT1 knockout mice. Further investigations aimed at unveiling the glycosylation pattern of LARGE should also be done, by using western blots for example. This will be a more problematic task seeing as there is now further evidence of that the binding of IIH6 is not as specific as thought (Lin et al., 2011).

CONCLUSION

This study has shown that upregulation of LARGE is not a viable treatment for DMD. Instead of preventing the development of muscular dystrophy, it increased the severity of it and advanced the onset of pathology. However, this does not exclude the possibility of LARGE proving to be a suitable treatment for dystroglycanopathies, a group of muscular dystrophies with a different cause.

In the scenario of LARGE becoming a treatment for the dystroglycanopathies, careful screening needs to be done of potential patients in order to exclude all patients suffering from DMD. The data presented in this study suggests that treating a DMD patient with LARGE would bring on disastrous results.

ACKNOWLEDGMENTS

I would first of all like to thank my supervisor at the Royal Veterinary College, Professor Dominic Wells, for his dedication to his students and his work, always prepared to calm us down when we worry too much.

Doctor Sofia Muses for putting up with my constant flow of questions and more worries, and being a thorough mentor when it comes to teaching GLP. Hannah Caneb, Rebecca Terry, Nazanin Rahmani and Charlotte Whitmore for their advice, but most of all for being good fun and always being prepared to take me out for a fun night. Dr Marta Fernandez-Fuente for making me practice my Spanish, Dr Maria Psatha for giving me a fight and adding some extra adrenalin to my day. Dr Mark Ackroyd for helping me with my western blots and putting up with my bad jokes, Professor Susan Brown for giving me advice and helping me get a hold of various articles. Dr Timothy Stone for his multilinguicity and teaching my brother physics in school.

Benjamin Alyoshkin for always being there for support and ventilation, Slawa Baumgart for always making me smile. Guy Davis for “stealing” our ice and giving me an excuse to take a break.

The rest of the neuromuscular group for making me feel welcome and part of the team!

Thank you to AstraZeneca for sponsoring my year in London and giving me the opportunity to meet such great people! Thank you to my supervisor at the Swedish University of Agricultural Science, Professor Stina Ekman, for choosing me to be part of this experience and helping me in the later stages of the process.

REFERENCES

- Barresi R, Michele DE, Kanagawa M, Harper HA, Dovico SA, Satz JS, Moore SA, Zhang W, Schachter H, Dumanski JP, Cohn RD, Nishino I, Campbell KP. (2004). LARGE can functionally bypass alpha-dystroglycan glycosylation defects in distinct congenital muscular dystrophies. *Nature Medicine*, vol. 10(7), ss. 696-703.
- Beltrán-Valero de Bernabé D, Currier S, Steinbrecher A, Celli J, van Beusekom E, van der Zwaag B, Kayserili H, Merlini L, Chitayat D, Dobyns WB, Cormand B, Lehesjoki AE, Cruces J, Voit T, Walsh CA, van Bokhoven H, Brunner HG. (2002). Mutations in the O-mannosyltransferase gene POMT1 give rise to the severe neuronal migration disorder Walker-Warburg syndrome. *The American Journal of Human Genetics*, vol 71(5), ss. 1033-43.
- Bodensteiner JB, Engel AG. (1987). Intracellular calcium accumulation in Duchenne dystrophy and other myopathies: a study of 567,000 muscle fibers in 114 biopsies. *Neurology*, vol 28(5), ss. 439-446.
- Brockington M, Torelli S, Prandini P, Boito C, Dolatshad NF, Longman C, Brown SC, Muntoni F. (2005). Localization and functional analysis of the LARGE family of glycosyltransferases: significance for muscular dystrophy. *Human Molecular Genetics*, vol 14(5), ss. 657-665.
- Brockington M, Torelli S, Sharp PS, Liu K, Cirak S, Brown SC, Wells DJ, Muntoni F. (2010) Transgenic overexpression of LARGE induces α -dystroglycan hyperglycosylation in skeletal and cardiac muscle. *PLoS One*, vol 5(12), e14434.
- Brockington M, Yuva Y, Prandini P, Brown SC, Torelli S, Benson MA, Herrmann R, Anderson LV, Bashir R, Burgunder JM, Fallet S, Romero N, Fardeau M, Straub V, Storey G, Pollitt C, Richard I, Sewry CA, Bushby K, Voit T, Blake DJ, Muntoni F. (2001). Mutations in the fukutin-related protein gene (FKRP) identify limb girdle muscular dystrophy 2I as a milder allelic variant of congenital muscular dystrophy MDC1C. *Human Molecular Genetics*, vol 10(25), ss. 2851-2859.
- Bulfield G, Siller WG, Wight PA, Moore KJ. (1984). X chromosome-linked muscular dystrophy (*mdx*) in the mouse. *Proceedings of the National Academy of Sciences U S A*, vol 81(4), ss.1189-1192.
- Cossu G, Mavilio F. (2000). Myogenic stem cells for the therapy of primary myopathies: wishful thinking or therapeutic perspective? *Journal of Clinical Investigation*, vol 105(12), ss. 1669-1674.
- Dubowitz V. (1982). The female carrier of Duchenne muscular dystrophy. *British Medical Journal (Clinical Research Edition)*, vol 284(6327), ss. 1423-1424.
- Emery AE. (2002). The muscular dystrophies. *Lancet*, vol 359(9307), ss. 687-695.
- Ervasti JM, Campbell KP. (1991) Membrane organization of the dystrophin-glycoprotein complex. *Cell*, vol 66(6), ss. 1121-1131.
- Grounds MD, Radley HG, Lynch GS, Nagaraju K, De Luca A. (2008). Towards developing standard operating procedures for pre-clinical testing in the *mdx* mouse model of Duchenne muscular dystrophy. *Neurobiology of Disease*, vol 31(1), ss.1-19.
- Hoffman EP, Brown RH Jr, Kunkel LM. (1987). Dystrophin: the protein product of the Duchenne muscular dystrophy locus. *Cell*, vol 51(6), ss. 919-928.

Kanagawa M, Nishimoto A, Chiyonobu T, Takeda S, Miyagoe-Suzuki Y, Wang F, Fujikake N, Taniguchi M, Lu Z, Tachikawa M, Nagai Y, Tashiro F, Miyazaki J, Tajima Y, Takeda S, Endo T, Kobayashi K, Campbell KP, Toda T. (2009). Residual laminin-binding activity and enhanced dystroglycan glycosylation by LARGE in novel model mice to dystroglycanopathy. *Human Molecular Genetics*, vol 18(4), ss. 621-631.

Khurana TS, Watkins SC, Chafey P, Chelly J, Tomé FM, Fardeau M, Kaplan JC, Kunkel LM. (1991). Immunolocalization and developmental expression of dystrophin related protein in skeletal muscle. *Neuromuscular Disorders*, vol 1(3), ss. 185-194.

Kobayashi K, Nakahori Y, Miyake M, Matsumura K, Kondo-Iida E, Nomura Y, Segawa M, Yoshioka M, Saito K, Osawa M, Hamano K, Sakakihara Y, Nonaka I, Nakagome Y, Kanazawa I, Nakamura Y, Tokunaga K, Toda T. (1998). An ancient retrotransposal insertion causes Fukuyama-type congenital muscular dystrophy. *Nature*, vol 394(6691), ss. 388-392.

Lefeber DJ, Schönberger J, Morava E, Guillard M, Huyben KM, Verrijp K, Grafakou O, Evangelidou A, Preijers FW, Manta P, Yildiz J, Grünwald S, Spilioti M, van den Elzen C, Klein D, Hess D, Ashida H, Hofsteenge J, Maeda Y, van den Heuvel L, Lammens M, Lehle L, Wevers RA. (2009). Deficiency of Dol-P-Man synthase subunit DPM3 bridges the congenital disorders of glycosylation with the dystroglycanopathies. *American Journal of Human Genetics*, vol 85(1), ss. 76-86.

Lin YY, White RJ, Torelli S, Cirak S, Muntoni F, Stemple DL. (2011). Zebrafish Fukutin family proteins link the unfolded protein response with dystroglycanopathies. *Human Molecular Genetics*, vol 20(9), ss. 1763-1775.

Longman C, Brockington M, Torelli S, Jimenez-Mallebrera C, Kennedy C, Khalil N, Feng L, Saran RK, Voit T, Merlini L, Sewry CA, Brown SC, Muntoni F. (2003). Mutations in the human LARGE gene cause MDC1D, a novel form of congenital muscular dystrophy with severe mental retardation and abnormal glycosylation of alpha-dystroglycan. *Human Molecular Genetics*, vol 12(21), ss. 2853-2861.

Lovering RM, Michaelson L, Ward CW. (2009). Malformed *mdx* myofibers have normal cytoskeletal architecture yet altered EC coupling and stress-induced Ca²⁺ signaling. *American Journal of Physiology - Cell Physiology*, vol 297(3), C571-580.

Martin PT, Xu R, Rodino-Klapac LR, Oglesbay E, Camboni M, Montgomery CL, Shontz K, Chicoine LG, Clark KR, Sahenk Z, Mendell JR, Janssen PM. (2009). Overexpression of Galgt2 in skeletal muscle prevents injury resulting from eccentric contractions in both *mdx* and wild-type mice. *American Journal of Physiology - Cell Physiology*, vol 296(3), C476-488.

Meryon E. (1852). On Granular and Fatty Degeneration of the Voluntary Muscles. *Medico-Chirurgical Transaction*, vol 35, ss. 73-84.1.

Michele DE, Barresi R, Kanagawa M, Saito F, Cohn RD, Satz JS, Dollar J, Nishino I, Kelley RI, Somer H, Straub V, Mathews KD, Moore SA, Campbell KP. (2002). Post-translational disruption of dystroglycan-ligand interactions in congenital muscular dystrophies. *Nature*, vol 418(6896), ss. 417-422.

Muntoni F, Torelli S, Brockington M. (2008). Muscular dystrophies due to glycosylation defects. *Neurotherapeutics*, vol 5(4), ss. 627-632.

Nguyen HH, Jayasinha V, Xia B, Hoyte K, Martin PT. (2002). Overexpression of the cytotoxic T cell GalNAc transferase in skeletal muscle inhibits muscular dystrophy in *mdx* mice. *Proceedings of the National Academy of Sciences U S A*, vol 99(8), ss. 5616-5621.

Ohlendieck K, Campbell KP. (1991). Dystrophin-associated proteins are greatly reduced in skeletal muscle from *mdx* mice. *Journal of Cell Biology*, vol 115(6), ss. 1685-1694.

Ohlendieck K, Matsumura K, Ionasescu VV, Towbin JA, Bosch EP, Weinstein SL, Sernett SW, Campbell KP. (1993). Duchenne muscular dystrophy: deficiency of dystrophin-associated proteins in the sarcolemma. *Neurology*, vol 43(4), ss. 795-800.

Salimena MC, Lagrota-Candido J, Quírico-Santos T. (2004). Gender dimorphism influences extracellular matrix expression and regeneration of muscular tissue in *mdx* dystrophic mice. *Histochemistry and Cell Biology*, vol 122(5), ss. 435-444.

Turner PR, Fong PY, Denetclaw WF, Steinhardt RA. (1991). Increased calcium influx in dystrophic muscle. *Journal of Cell Biology*, vol 115(6), ss. 1701-1712.

van Reeuwijk J, Janssen M, van den Elzen C, Beltran-Valero de Bernabé D, Sabatelli P, Merlini L, Boon M, Scheffer H, Brockington M, Muntoni F, Huynen MA, Verrips A, Walsh CA, Barth PG, Brunner HG, van Bokhoven H. (2005). POMT2 mutations cause alpha-dystroglycan hypoglycosylation and Walker-Warburg syndrome. *Journal of Medical Genetics*, vol 42(12), ss. 907-912.

Whitehead NP, Yeung EW, Allen DG. (2006). Muscle damage in *mdx* (dystrophic) mice: role of calcium and reactive oxygen species. *Clinical and Experimental Pharmacology and Physiology*, vol 33(7), ss. 657-662.

Yoshida A, Kobayashi K, Manya H, Taniguchi K, Kano H, Mizuno M, Inazu T, Mitsuhashi H, Takahashi S, Takeuchi M, Herrmann R, Straub V, Talim B, Voit T, Topaloglu H, Toda T, Endo T. (2001). Muscular dystrophy and neuronal migration disorder caused by mutations in a glycosyltransferase, POMGnT1. *Developmental Cell*, vol 1(5), ss. 717-724.

Zhang Z, Zhang P, Hu H. (2011). LARGE Expression Augments the Glycosylation of Glycoproteins in Addition to α -Dystroglycan Conferring Laminin Binding. *PLoS One*, vol 6(4), e19080.

APPENDIX

Appendix 1. Counts done on myofibres in *mdx* and LV5/*mdx*. *Mdx* mice in bold typing, LV5/*mdx* in normal typing. The LV5/*mdx* show a higher number in average total fibre count, and a lower percentage of non-centrally nucleated fibres in all animals when comparing with the *mdx* animals

Sample	1st count	2nd count	3rd count	Average non-centralized	Tot fibers	% Within group
10/474	373	433	396	400.7	5380	7.7
10/478	402	381		391.5		7.5
10/482	203	240		221.5		3.4
10/486	173	287	242	234		4.5
10/490	170	174		172		2.7
10/494	336	409	402	382.3	4725	7.3
11/3	199	191		195	8337	3.0
11/7	138	148		143	5402	2.2
11/11	187	180		183.5		2.8
11/15	476	472		474	5535	9.1
11/19	324	315		319.5		6.1
11/23	132	95	126	117.7	5712	1.8

Average <i>mdx</i>	5,213.3	7.0
Average LV5/ <i>mdx</i>	6,483.7	2.7